Coral Reef Island Initiation and Development Under Higher Than Present Sea Levels

H. K. East[1,2], C. T. Perry[2], P. S. Kench[3,4], Y. Liang[4,5], and P. Gulliver[6]

[1]Department of Geography and Environmental Sciences, Northumbria University, Newcastle upon Tyne, UK.

[2]Geography, College of Life and Environmental Sciences, University of Exeter, Exeter, UK.

[3]Department of Earth Science, Simon Fraser University, British Columbia, Canada.

[4]School of Environment, University of Auckland, Auckland, New Zealand.

[5]Faculty of Health, Humanities, and Computing, Southern Institute of Technology, Invercargill, New Zealand.

[6]NERC Radiocarbon Facility, Scottish Enterprise Technology Park, East Kilbride, UK.

Corresponding author: Holly East (holly.east@northumbria.ac.uk)

Key Points:

- Intra-regional differences exist in the timings and modes of Maldivian atoll rim reef island initiation and development.
- Evidence of Maldivian rim reef island formation under higher than present sea levels.
- Future sea-level rise may reactivate the process regime responsible for reef island formation, resulting in vertical island-building.

Abstract

Coral reef islands are considered to be among the most vulnerable environments to future sea-level rise. However, emerging data suggest that different island types, in contrasting locations, have formed under different conditions in relation to past sea level. Uniform assumptions about reef island futures under sea-level rise may thus be inappropriate. Using chronostratigraphic analysis from atoll rim islands (sand- and gravel-based) in the southern Maldives, we show that whilst island building initiated at different times around the atoll (~2,800 cal. yr. B.P. and ~4,200 cal. yr. B.P. at windward and leeward rim sites respectively), higher than present sea levels and associated high-energy wave events were actually critical to island initiation. Findings thus suggest that projected sea-level rise and increases in the magnitude of distal high-energy wave events could reactivate this process regime which, if there is an appropriate sediment supply, may facilitate further vertical reef island-building.

Plain Language Summary

The habitability of reef island nations under climate change is a debated and controversial subject. Improving understanding of reef island responses to past environmental change provides important insights into how islands may respond to future environmental change. It is typically assumed that all reef islands will respond to environmental change in the same manner, but such assumptions fail to acknowledge that reef islands are diverse landforms that have formed under different sea-level histories and across a range of settings. Here, we reconstruct reef island evolution in two contrasting settings (in terms of exposure to open ocean swell) in the southern Maldives. Important differences in island development are evident between these settings in the timings, sedimentology and modes of island building, even at local scales. This implies that island responses to climate change may be equally diverse and site-specific. We present evidence that island initiation was associated with higher than present sea levels and high-energy wave events. Projected increases in sea level, and the magnitude of such high-energy wave events could therefore recreate the environmental conditions under which island formation occurred. If there is a suitable sediment supply, this could result in vertical island-building which may enhance reef island future resilience.

1 Introduction

Coral reef islands are low-lying (<3 m above mean sea level, MSL) accumulations of wave-deposited bioclastic sediment. As a function of their low elevations, small areal extents and largely unconsolidated structures, they are frequently perceived to be among the most vulnerable environments to climate change, particularly to sea-level rise (IPCC, 2014). There is thus major concern over the future existence and habitability of atoll nations (Dickinson, 2009; Storlazzi et al., 2015, 2018), within which reef islands provide the only habitable land. To assess the future of atoll nations, it is therefore critical to understand the timings, modes of, and controls on island development, especially in the context of past sea levels and inferred wave energy regimes. However, there is a paucity of reef island chronostratigraphic research upon which to make confident projections of island trajectories that can accommodate for the diversity of island settings. While an increasing number of studies are examining island planform adjustments over decadal timescales (Aslam & Kench, 2017; Duvat et al., 2017; Kench et al., 2015, 2018), such knowledge needs to be integrated with a more comprehensive understanding of island responses to longer-term (millennial timescale) environmental changes, particularly in sea level. Existing chronostratigraphic datasets indicate that marked inter-regional differences exist in reef island

development histories (Perry et al., 2011), but it is knowledge of intra-regional variability that is needed to support more robust national-scale reef island vulnerability assessments.

The Maldives provides an especially interesting region in which to examine such intra-regional variability because of the diversity of island types and settings. In this context, there is growing understanding of intra-regional differences in Maldivian reef island development on small annular reef platforms, locally termed 'faro' (Kench et al., 2005; Perry et al., 2013). However, detailed understanding of when and how islands form on linear rim platforms (reef platforms around atoll perimeters) in the Maldives is essentially non-existent. This knowledge gap is highly significant for predicting scenarios of future reef island change because, in the Maldives, the rim island types dominate spatially (82.4% of land area), host the majority of the population (88.9%), and therefore support the nation's key infrastructure (all regional capitals, hospitals and 'safe islands'). Furthermore, there are many reasons to support the hypothesis that modes and timings of island development differ between linear rim platform and faro settings. Specifically, there are distinct differences between these settings in hydrodynamic process regimes (Kench et al., 2006), sediment production rates (Perry et al., 2015, 2017), and platform morphologies.

Here, we report detailed morphostratigraphic analyses and AMS radiocarbon dating from reef islands (sand- and gravel-based) on windward and leeward aspects of Huvadhoo Atoll rim. Collectively, these datasets are used to construct a new conceptual model of Maldivian rim island development, and thus to identify key phases of island building, their timings, modes of sedimentation, and relationships to past sea-level change. In this context, sea level in this region is interpreted to have risen steadily in the post-glacial period, reaching present levels by ~4,500 cal. yr. B.P.. A period of higher than present sea level (of at least ~0.5 m above contemporary MSL) then occurred between 4,000 and 2,100 cal. yr. B.P., before falling to its present level (Kench et al., 2009). Our datasets highlight intra-regional differences and similarities in reef island development since sea level first reached its current level in the mid-Holocene. These data suggest there have been marked differences in the modes and timings of island development on linear rim platforms and faros in the region.

2 Field setting and methodology

The reef systems of the Maldives archipelago support ~1,200 reef islands inhabited by a population of ~417,000. Satellite altimetry data show oceanic swell waves approach from south-easterly directions between November and March (northeast monsoon), and south to south-westerly directions between April and November (westerly monsoon; Young, 1999). Wave energies during the westerly monsoon are greater than those during the northeast monsoon (Young, 1999; Kench & Brander, 2006). Our study focused on two sites on Huvadhoo Atoll rim, which represent end-members with respect to relative exposure to open ocean swell: a north-eastern leeward site (Galamadhoo and Baavanadhoo islands), and a south-western windward site (Mainadhoo, Boduhini and Kudahini islands; Figure 1). To characterize the oceanic process regime, WaveWatch III model hindcasts (Durrant et al., 2013; Tolman, 2009) were undertaken for the period 1979 to 2010 at locations 20 km off the oceanward platform margin at each site. Significant wave height (H_s) and dominant wave period (T_O) were significantly higher and longer at the windward than the leeward site respectively (paired t-tests; P = <0.001). At the windward site, H_s = 1.6 ± 0.4 m and T_O = 10.0 ± 1.6 s. At the leeward site H_s = 1.4 ± 0.4 m and T_O = 9.7 ± 1.5 s (n = 279,768 for each parameter at each site; Figure S1). The maximum tidal range (lowest to highest astronomical tides) in the southern Maldives is 1.4 m (Woodroffe, 1993).

Island topographic surveys were undertaken using a laser level along 11 platform-island transects (instrument accuracy = ±1.5 mm, but, given inherently imperfect field conditions, we suggest a conservative error of ±1 cm). Each transect started and terminated on the reef flat in areas of live coral growth. Topographic data were corrected to height above MSL using tide tables for Gan (00°41’ S, 73°9’ E) from the University of Hawaii Sea Level Centre. Island planform was surveyed using GPS. Subsurface stratigraphy along each transect was determined by percussion coring (n = 28; Figure 2). Core recovery was 100%, with an average length of 2.31 m. From each core, one sample (150 g) from each facies was recovered for textural and compositional analyses (n = 119; descriptive nomenclature of Udden-Wentworth is used throughout). Ground penetrating radar (GPR; Geophysical Survey Systems SIR2000 system with a monostatic 200 MHz shielded antenna) traces were obtained from 280 m of transects to further characterize subsurface stratigraphy. To determine island chronologies, 40 samples were selected for accelerator mass spectrometry (AMS) radiocarbon dating. To minimize the temporal disparity between time of death of the organism and its deposition, microscopic screening was

undertaken to select only pristine samples (Kench et al., 2014; Woodroffe et al., 2007). A variety of materials were therefore dated, including coral clasts, foraminifera, *Halimeda* segments and gastropod shells (Text S1; Table S1).

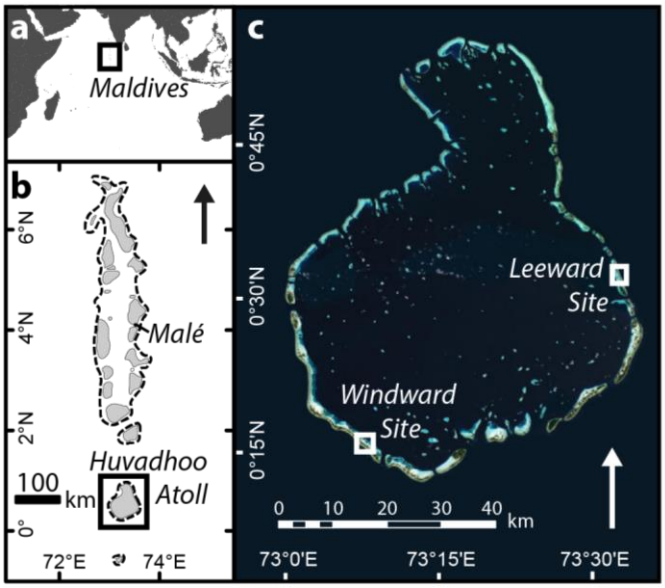

Figure 1. Location of the Maldives (a); Huvadhoo Atoll (b); and windward and leeward study sites (c).

3 Results

Island morphologies are comparable within windward and leeward sites, but there are marked differences between these settings. Windward islands are characterized by steep unconsolidated peripheral oceanward rubble ridges (<2 m above MSL), consolidated conglomerate platforms at their oceanward margins, but low overall elevations (excluding marginal ridges, average = ~0.81 m above MSL; Figures 2, S2 and S3). In contrast, leeward islands are characterized by extensive beachrock outcrops at island margins (<25 m wide, <550 m long), stranded beachrock (extending <~230 m), no marked peripheral ridges, and higher overall island elevations (average = ~1.44 m above MSL; Figures 2, S3 and S4).

Of 28 cores, 27 terminated below the elevation of live coral growth (~0.5 m below MSL). A high proportion (19) terminated in unconsolidated sediment, while 8 (all close to the oceanward island margins) terminated on a hard reef surface, interpreted as the underlying reef flat. This indurated surface does not occur in lagoonward cores, suggesting that the underlying reef flat slopes towards the atoll lagoon. Island sedimentary composition was highly consistent

between islands and sites. Coral was the dominant constituent (76.6 ± 0.6%), with lesser proportions of crustose coralline algae (11.0 ± 0.3%) and molluscs (8.8 ± 0.5%). However, three distinct facies and four sub-facies were identified primarily on the basis of textural characteristics (described in detail in East et al., 2016; Tables S2 and S3). Facies 1 comprised organically enriched (i.e. penetrated by broken plant remains) coarse-grained sand, which occurred in the upper ~<50 cm of cores. Facies 2 was a predominantly sand-grade unit, differentiated as being medium- and coarse-grained in sub-facies 2A and 2B respectively. Facies 2 underlay Facies 1 and was dominant in leeward cores (thickness <2 m). GPR data show Facies 2 stratigraphy to be lagoonward-dipping, indicative of progradational lagoon infill deposits (Figures 3 and S5). Facies 3, a clast-supported unit characterized by the prevalence of rubble, underlay Facies 2. A subdivision between 3A and 3B was based on an increase in rubble size whereby clasts were up to pebble- and cobble-grade in 3A and 3B respectively (longest axes = <4 cm in 3A and <12 cm in 3B; *i.e.* as large as could be recovered given that core diameter = 9 cm). Facies 3 was most prevalent on the windward rim (thickness <2 m). Throughout cores, proportions of gravel-sized material were significantly higher on the windward than the leeward rim ($P = 0.003$; one-way analysis of variance, ANOVA).

Reef island chronologies were reconstructed using AMS radiocarbon dates (Table S1, Figures 2 and 4). The oldest radiometric dates were from the underlying reef flat: *c.* 3,600 to 2,800 cal. yr. B.P., and *c.* 4,450 cal. yr. B.P. in windward and leeward settings respectively. Above the underlying reef flat, the oldest dates (i.e. of reef island initiation) were *c.* 2800 cal. yr. B.P. and *c.* 4,200 cal. yr. B.P. on the windward and leeward rims respectively. Dates from the Facies 2-3 interface were relatively consistent (*c.* 1,800 to 1,500 cal. yr. B.P) at both sites. The youngest dates in both rim settings were found towards lagoonward island margins (*c.* 640 and 524 cal. yr. B.P.).

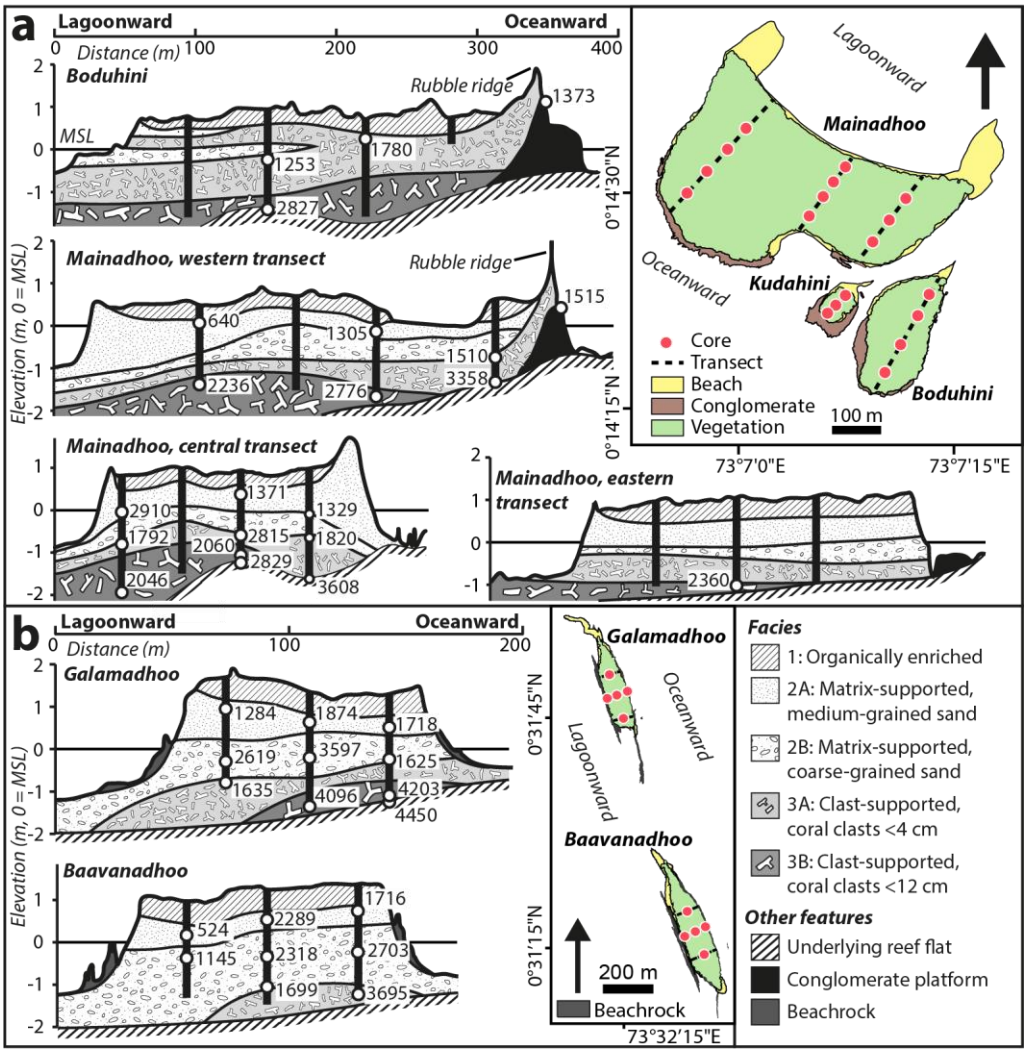

Figure 2. Topographic cross-sections, planform surveys, core logs, and median radiometric dates from (a) the two main windward islands (the profile for Kudahini is provided in Figure S2), (b) the central transects of both leeward islands (the northern and southern transects of Galamadhoo and Baavanadhoo are provided in Figure S4).

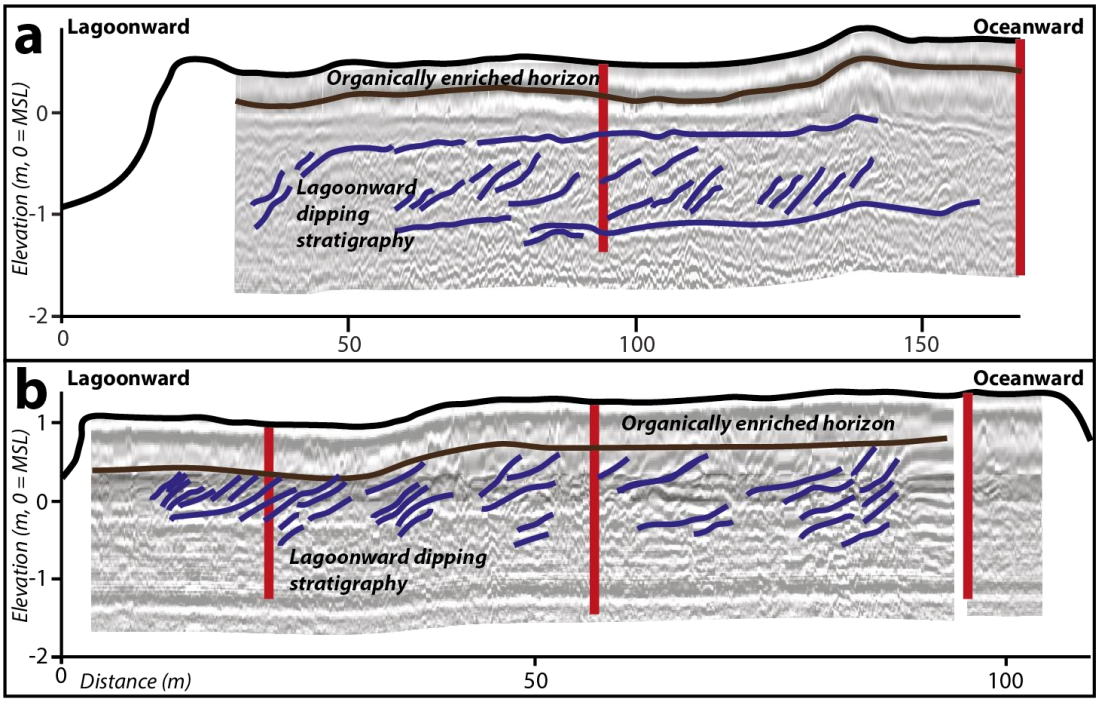

Figure 3. GPR traces from the windward rim (a: western transect of Mainadhoo) and leeward rim (b: central transect of Baavanadhoo). Red lines represent core locations.

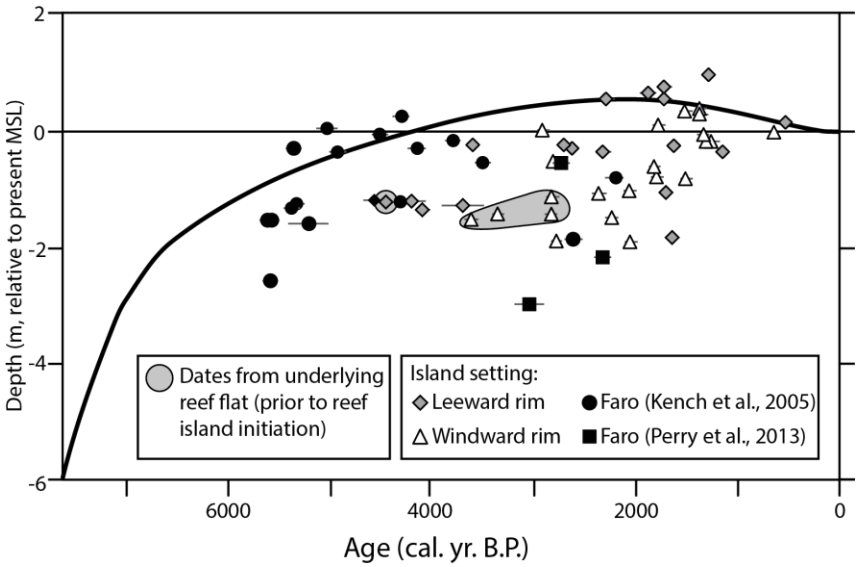

Figure 4. Age-elevation plot with reef island radiocarbon dates from the present study and faro reef platforms (Kench et al., 2005; Perry et al., 2013). Horizontal error bars show the 63.8% probability range of calibrated dates. Datasets are shown relative to Kench et al.'s (2009) sea-level curve for the Maldives.

4 Model of island formation

On the basis of island morphologies, cores, sedimentary facies, GPR traces and radiocarbon dates, a new conceptual model of Maldivian atoll rim reef island development can be proposed (Figure 5). We believe that the data provide sufficient evidence to suggest this may be an appropriate model for reef islands on linear rim platforms throughout the Maldives. This is a model that can also be tested in other areas, particularly, given comparable sea-level histories, in the central Indian Ocean. Dates from the underlying reef flat (*c*. 3,600 to 2,800 cal. yr. B.P., 1.1 to 1.5 m below MSL, and *c*. 4,450 cal. yr. B.P., 1.21 m below MSL, on the windward and leeward rim respectively) correspond to a time when sea level was approaching present levels (Gischler et al., 2008; Kench et al., 2009; Figure 4). These dates are interpreted as defining the period within which vertical reef growth was the dominant constructive process (*Stage A*), which is broadly consistent with the timeframes suggested by Woodroffe et al. (1993) and Kench et al. (2009).

Island initiation then occurred through accumulation of unconsolidated rubble-dominated material (cobble- and, subsequently, pebble-sized clasts; Facies 3) immediately above the former reef flat (*Stage B*). Successive high magnitude events likely pushed the rubble deposits across the reef platform surface to provide the basement for island formation. This comprised part of a continuum of platform ('bucket' style) infilling, a mode of carbonate platform evolution in which sediment derived from the carbonate-productive fore-reef and reef flat infills lagoons (Purdy & Gischler, 2005). This phase of rubble accumulation occurred between *c*. 2,800 and 1,800 cal. yr. B.P. on the windward rim, and *c*. 4,200 and 1,600 cal. yr. B.P. on the leeward rim, and is congruent with a period when sea level is reported to have been approximately 0.5 m above present (Kench et al., 2009; Figure 4). Such higher sea levels would have enabled higher wave energies to propagate across reef flats, resulting in increased rates of rubble generation (via physical erosion) and transport. At this time, water depths on the adjacent reef flats (~1 m below MSL) would have been conducive to coral growth and evidence of emergent reef build-ups from this time indicate that coral cover was likely high (Kench et al., 2009). While island initiation at both sites occurred via rubble accumulation, modes of deposition differed between settings. On the windward rim, comparatively thick (up to ~2 m) rubble sheets were deposited which appear to extend below the entirety of the windward islands. No dateable material could be obtained from the oceanward rubble ridges but, given the large clast sizes of material on the ridges (<0.8

m diameter), they may have been deposited during this stage. Similarly, the upper surface of the conglomerate platform was dated *c*. 1,400 cal. yr. B.P and was thus likely deposited and cemented at this time. This conglomerate may have aided island formation by providing a low energy leeward depocentre. In contrast, on the leeward rim, a rubble bank was deposited, which dips lagoonward and was relatively thin (up to ~0.85 m). The thin vertical extent of this deposit likely results from the leeward rim being less exposed to oceanic swell. High magnitude events, with capacity for rubble generation and transport, would therefore have been less frequent than on the windward rim. In addition, the leeward islands are located further (~540 m) from their oceanward platform margin than the windward islands (~250 m), the most likely source of rubble-grade material. The leeward rubble bank was below MSL and, in the absence of a conglomerate platform to anchor deposits, it is likely that the leeward islands were more mobile.

Following the deposition of these rubble-dominated sequences, sand accumulation (Facies 2) became the dominant constructive process (*Stage C*). At the timing of the switch from Stage B to C (*c*. 1,800 to 1,500 cal. yr. B.P.) sea level was falling toward contemporary levels and thus the high-energy window closed (Kench et al., 2009; Figure 4). Hence, there would have been a progressive reduction in wave energy and, in turn, rubble generation and transport. The dominant mode of accretion was likely lateral lagoonward progradation. This interpretation is supported by radiocarbon dates, which are generally younger toward the lagoonward island margins, and the strong lagoonward-dipping reflectors in GPR traces (Figures 3 and S5). As rubble deposits attained higher elevations along oceanward island margins, rubble may have blocked oceanward-lagoonward cross-rim sediment transport and thus Facies 2 was likely derived from the lagoonward marine environment. Rates of lagoonward island progradation were likely highest on the leeward rim due to the dominant westerly wind direction and, hence, the long fetch distance (~60 km) across the atoll lagoon. With westerly propagation of wind-driven wave energy across the atoll lagoon, lagoonal wave energy was at a maximum at the leeward site. This may account for the greater thickness of Facies 2 and the higher elevation of the leeward islands. The youngest dates were *c*. 500-600 cal. yr. B.P, which suggests an organically enriched horizon has developed (Facies 1) and vegetation growth has occurred (*Stage D*) since this time.

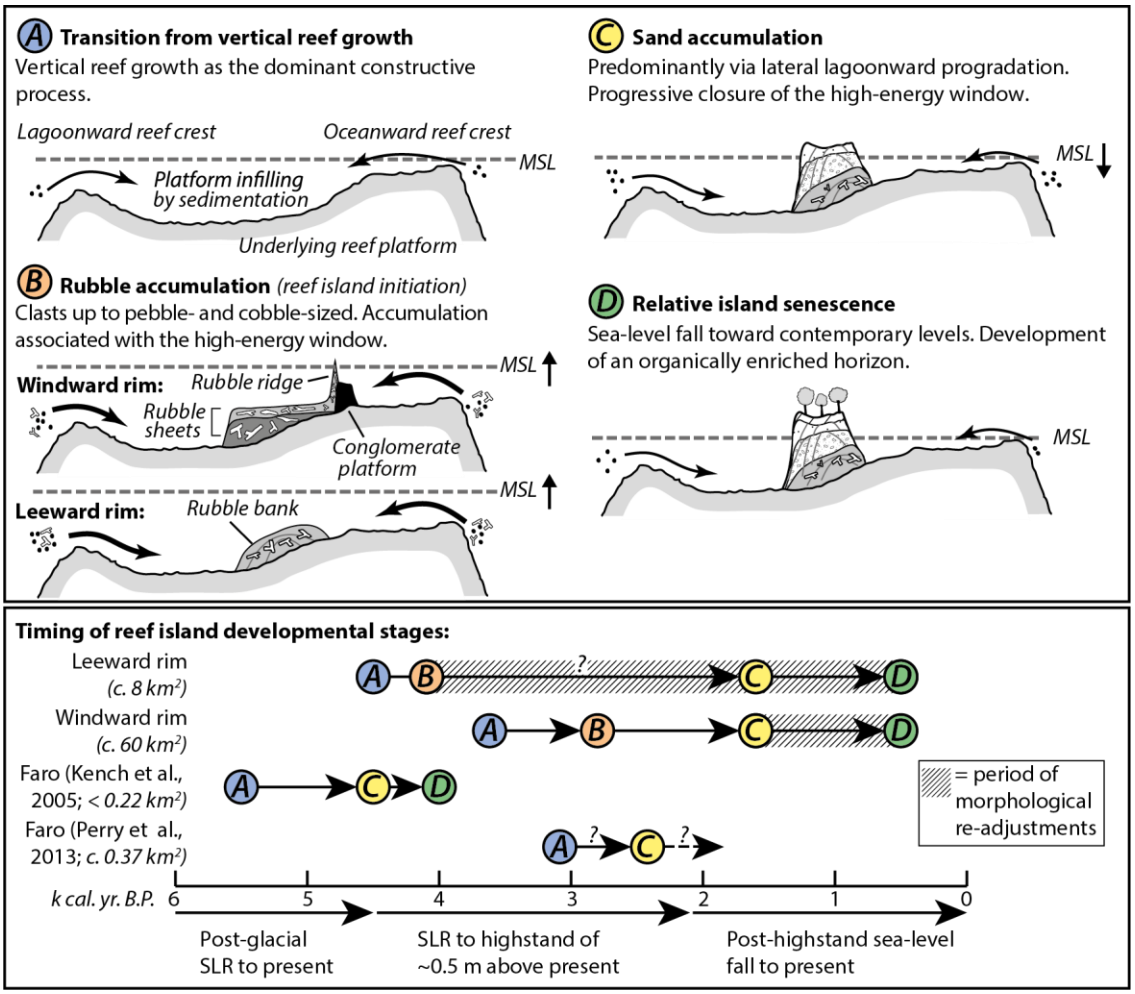

Figure 5. Conceptual model of Maldivian reef rim island development and relation to Holocene sea-level history (Kench et al., 2009). Approximate reef platform areas provided for reference.

5 Evidence of island planform adjustments

As is common in reef island chronostratigraphic studies, we note a number of age inversions in our core records. This is typically a function of the highly dynamic nature of reef island formation (Kench et al., 2015), and thus dates are interpreted as windows of island accumulation rather than definitive time periods. Age inversions are likely due to sediment redeposition, which may occur within (i) the marine environment prior to island deposition; and/or (ii) the island itself due to reworking of the sediment reservoir. As dates were only obtained on pristine samples (Text S1), age inversions are most likely due to the latter. On the windward rim, Stage B may thus have been a period of increased sediment mobility (Figure 5). All windward site age inversions were on the central transect of Mainadhoo. We thus

hypothesize that Mainadhoo was initially two separate islands which coalesced along this transect. Coalescence may have occurred through 'roll-around' of older, preferentially sand-sized, material from the separate islands by alongshore sediment fluxes to fill the inter-island passage and weld the islands through embayment infilling (Kench et al., 2015). This is supported by the presence of a sandy bay, as opposed to a rubble ridge, and the absence of conglomerate on the oceanward margin of this transect.

On the leeward rim, we suggest islands have undergone morphological adjustments throughout Stages B to D (Figure 5). This is indicated by age inversions in 3 of 6 dated cores, the consistency of the Facies 2-3 interface dates, and extensive beachrock outcrops. Reworking may have occurred via 'rollover' whereby material was eroded from the oceanward island margin and redeposited toward the lagoonward coast (Woodroffe et al., 1999). The greater mobility of leeward, rather than windward, islands is consistent with prior work, which found sand-based islands to be more mobile than rubble-based islands (Kench et al., 2015). The ongoing existence of highly mobile islands is contingent upon reworking of the original island core and/or generation of new sediment. Due to their apparently greater mobility, leeward rim islands could thus be more vulnerable to climate change than their windward counterparts as a larger sediment supply may be required to maintain island volumes.

6 Discussion

Our findings demonstrate clear intra-regional variations in the timings, sedimentology and modes of rim reef island development in the Maldives. This local-scale variability has implications for reef island systems globally as it renders construction of unifying models of island evolution problematic. Notably, there were marked differences in the timing of island initiation between windward (*c*. 2,800 cal. yr. B.P.) and leeward (*c*. 4,200 cal. yr. B.P.) rim settings. Furthermore, Kench et al. (2005) found faro island formation (South Maalhosmadulu Atoll, northern-central Maldives) occurred between 5,500 and 4,000 yr. B.P.. Hence, the key phase of faro island building occurred under lower than present sea levels (Kench et al., 2005), whereas the key phase of island building in this study occurred under higher than present sea levels (Figure 4). A key consistency between rim settings was the timing of the switch from rubble to sand accumulation, which is congruent with the closure of the high energy window following the mid-to-late Holocene sea-level highstand (Kench et al., 2009). Given that these

differences are intra-regional, and thus exist under comparable sea-level histories, this highlights that sea level is not the sole control on island formation, as is implicated in perceptions of their vulnerability. Hence, reef islands are able to form at different stages of sea-level rise, fall and stabilization (Figure 4).

One likely driver of these intra-regional island age differences is reef platform size, as has been proposed for faro islands in the Maldives (Perry et al., 2013). This is because the earlier a platform infills, the earlier an underlying substrate is available for island formation, and thus larger platforms require longer time periods to infill. Our data suggest similar factors may strongly influence the formation of atoll rim islands given that the windward platform is markedly larger (~60 km^2) than the leeward platform (~8 km^2). Such differences in island ages may be exacerbated by differences in sediment production rates, which are higher on faro than linear rim platforms due to their differing eco-geomorphic zonations. Faros are entirely encircled by a highly productive reef crest (Perry et al., 2015), whereas these high productivity zones only occur on the lagoonward and/or oceanward margins of rim platforms (Perry et al., 2017).

Fundamental intra-regional differences were also found in the modes of reef island development. Firstly, the lateral lagoonward mode of sand accumulation differs strikingly from the faro model of reef island development, in which islands accrete from a central core (Kench et al., 2005). This is likely a function of differences in hydrodynamic process regimes whereby linear rim platforms are characterized by strong cross-platform wave energy gradients, whereas waves converge at a focal point on faro surfaces as wave energy is incident around 360° of their platform margins. Secondly, the mechanisms of island initiation differ between faro and linear rim platform islands. Linear rim island initiation occurred with rubble accumulation, whereas faro island initiation was associated with low energy sedimentation (Kench et al., 2005). As rubble generation and transport necessitate high wave energies, this also reflects their distinctly different hydrodynamic process regimes. In addition, the greater prevalence of rubble in linear rim islands highlights the differential roles of biological and physical processes in island formation whereby faro island building is more dependent on biological processes than rim island building. Given the close proximity of the Maldives to the equator and the rarity of storm events with cyclone intensities (Woodroffe, 1993), rubble generation and transport were likely facilitated by long period high-energy swell events driven by high latitude storms (Hoeke et al., 2013). Such distal high-energy swell events have previously inundated islands in Huvadhoo

Atoll (UNDP, 2007) and there may, as in other regions, have been higher intensity storms during the Holocene (Nott & Forsyth, 2012). Given the key role of long period distal swell events in island initiation, there are important resultant implications for island trajectories under climate change. The largest future increases in wave activity have been projected to occur within the Southern Ocean with increased northerly propagation of swell (Hemer et al., 2013). Hence, the magnitude of long period swell events may increase, which could cause additional reef rim island accretion and planform change.

While climate change projections (Table S4) may produce hydrodynamic conditions that are conducive to island building, it is pertinent to note several caveats to this optimistic prognosis. Firstly, island accretion is contingent upon the availability of a suitable sediment supply. As islands are formed predominantly of coral (Table S3), the presence of live coral in the adjacent reef communities (and the processes that denude coral into sand-grade sediment) will be a necessity for ongoing island resilience. However, this could be problematic as corals face a range of threats under climate change, including increases in ocean acidity and sea surface temperatures (IPCC, 2014). Secondly, island building within the present study has occurred over millennial temporal scales, but it is decadal to centennial temporal scales that are of most interest to the inhabitants of atoll nations. Thirdly, the high-energy overwash events that will drive island accretion, along with likely shifts in island planform, may devastate atoll nations' infrastructure, potentially compromising island habitability in its current form. A challenge for atoll nations is thus to develop infrastructure with the capacity to withstand or be adaptable to such high-energy events.

7 Conclusions

We present a new conceptual model of reef island evolution for linear atoll rim platform settings in the Maldives. Our data demonstrate that marked intra-regional differences exist in island morphology, stratigraphy and timings of initiation, even at the scale of an individual atoll. In addition to the model of faro reef island development in the region (Kench et al., 2005), we present evidence that rim islands formed under higher than present sea levels and distal high-energy wave events. Projections of future sea-level rise and increases in the magnitude of distal high-energy wave events may thus reactivate this process regime, which, if there is a suitable sediment supply, could result in further island building and remobilization. This could enhance

reef island resilience by facilitating vertical island accretion. In addition to sea level and distal high-energy wave events, we suggest reef platform size and hydrodynamic process regime represent key influences on intra-regional variability in island evolution. These findings thus have implications for the future adaptive capacity of atoll nations globally. Specifically, the challenge is to incorporate intra-regional diversity in reef island evolution into national-scale vulnerability assessments.

Acknowledgments

We thank Mohamed Aslam (LaMer) for facilitating fieldwork. This work was supported by a NERC PhD studentship (NE/K500902/1). Radiocarbon dates were funded through allocation 1853.1014 from the Natural Environment Research Council (UK). Data are available within the Supplementary Information and will be made available on Northumbria University's institutional repository (nrl.northumbria.ac.uk) upon publication.

References

Aslam, M., & Kench, P. S. (2017). Reef island dynamics and mechanisms of change in Huvadhoo Atoll, Republic of Maldives, Indian Ocean. *Anthropocene*, *18*, 57–68. https://doi.org/10.1016/j.ancene.2017.05.003

Dickinson, W. R. (2009). Pacific atoll living: How long already and until when. *GSA Today*, *19*(3), 4–10. https://doi.org/10.1130/GSATG35A.1

Durrant, T., Hemer, M., Trenham, C., & Greenslade, D. (2013). *CAWCR Wave Hindcast 1979-2010* (v5). CSIRO. https://doi.org/10.4225/08/523168703DCC5

Duvat, V. K. E., Salvat, B., & Salmon, C. (2017). Drivers of shoreline change in atoll reef islands of the Tuamotu Archipelago, French Polynesia. *Global and Planetary Change*, *158*, 134–154. https://doi.org/10.1016/j.gloplacha.2017.09.016

East, H. K., Perry, C. T., Kench, P. S., & Liang, Y. (2016). Atoll-scale comparisons of the sedimentary structure of coral reef rim islands, Huvadhu Atoll, Maldives. *Journal of Coastal Research*, 577–581. https://doi.org/10.2112/SI75-116.1

Ford, M. R., & Kench, P. S. (2012). The durability of bioclastic sediments and implications for coral reef deposit formation. *Sedimentology*, *59*(3), 830–842. https://doi.org/10.1111/j.1365-3091.2011.01281.x

Freeman, S., Bishop, P., Bryant, C., Cook, G., Dougans, D., Ertunc, T., et al. (2007). The SUERC AMS laboratory after 3 years. *Nuclear Instruments and Methods in Physics Research Section B: Beam Interactions with Materials and Atoms*, *259*(1), 66–70. https://doi.org/10.1016/j.nimb.2007.01.312

Gischler, E., Hudson, J. H., & Pisera, A. (2008). Late Quaternary reef growth and sea level in the Maldives (Indian Ocean). *Marine Geology*, *250*(1), 104–113. https://doi.org/10.1016/j.margeo.2008.01.004

Hemer, M. A., Fan, Y., Mori, N., Semedo, A., & Wang, X. L. (2013). Projected changes in wave climate from a multi-model ensemble. *Nature Climate Change*, *3*(5), 471–476. https://doi.org/10.1038/nclimate1791

Hoeke, R. K., McInnes, K. L., Kruger, J. C., McNaught, R. J., Hunter, J. R., & Smithers, S. G. (2013). Widespread inundation of Pacific islands triggered by distant-source wind-waves. *Global and Planetary Change*, *108*, 128–138. https://doi.org/10.1016/j.gloplacha.2013.06.006

IPCC (2014). *Climate Change 2014: Synthesis Report— Contribution of Working Groups I, II and III to the Fifth Assessment Report of the IPCC*. (Pachauri, R. K., & Meyer, L. A., Eds.) 151 pp., IPCC, Geneva, Switzerland.

Kench, P .S. & Brander, R. W. (2006). Response of reef island shorelines to seasonal climate oscillations: South Maalhosmadulu atoll, Maldives. *Journal of Geophysical Research: Earth Surface*, *111*(F1). https://doi.org/10.1029/2005JF000323

Kench, P. S., Brander, R. W., Parnell, K. E., & McLean, R. F. (2006) Wave energy gradients across a Maldivian atoll: implications for island geomorphology. *Geomorphology*, *81*, 1–17. https://doi.org/10.1016/j.geomorph.2006.03.003

Kench, P. S., McLean, R. F., & Nichol, S. L. (2005). New model of reef-island evolution: Maldives, Indian Ocean. *Geology*, *33*(2), 145–148. https://doi.org/10.1130/G21066.1

Kench, P. S., Smithers, S. G., McLean, R. F., & Nichol, S. L. (2009). Holocene reef growth in the Maldives: Evidence of a mid-Holocene sea-level highstand in the central Indian Ocean. *Geology*, *37*(5), 455–458. https://doi.org/10.1130/G25590A.1

401 Kench, P. S., Thompson, D., Ford, M. R., Ogawa, H., & McLean, R. F. (2015). Coral islands
402 defy sea-level rise over the past century: Records from a central Pacific atoll. *Geology*, *43*(6),
403 515–518. https://doi.org/10.1130/G36555.1

404 Kench, P. S., Owen, S. D., & Ford, M. R. (2014). Evidence for coral island formation during
405 rising sea level in the central Pacific Ocean. *Geophysical Research Letters*, *41*(3), 820–827.
406 https://doi.org/10.1002/2013GL059000

407 Kench, P. S., Ford, M. R., & Owen, S. D. (2018). Patterns of island change and persistence offer
408 alternate adaptation pathways for atoll nations. *Nature Communications*, *9*(1), 605.
409 https://doi.org/10.1038/s41467-018-02954-1

410 Nott, J., & Forsyth, A. (2012). Punctuated global tropical cyclone activity over the past 5,000
411 years. *Geophysical Research Letters*, *39*(14). https://doi.org/10.1029/2012GL052236

412 Perry, C. T., Kench, P. S., Smithers, S. G., Yamano, H., O'Leary, M., & Gulliver, P. (2013).
413 Time scales and modes of reef lagoon infilling in the Maldives and controls on the onset of
414 reef island formation. *Geology*, *41*(10), 1111–1114. https://doi.org/10.1130/G34690.1

415 Perry, C. T., Kench, P. S., O'Leary, M. J., Morgan, K. M., & Januchowski-Hartley, F. (2015).
416 Linking reef ecology to island building: Parrotfish identified as major producers of island-
417 building sediment in the Maldives. *Geology*, *43*(6), 503–506.
418 https://doi.org/10.1130/G36623.1

419 Perry, C. T., Kench, P. S., Smithers, S. G., Riegl, B. R., Gulliver, P., & Daniells, J. J. (2017).
420 Terrigenous sediment-dominated reef platform infilling: an unexpected precursor to reef
421 island formation and a test of the reef platform size–island age model in the Pacific. *Coral*
422 *Reefs*, *36*(3), 1013–1021. https://doi.org/10.1007/s00338-017-1592-7

423 Perry, C. T., Kench, P. S., Smithers, S. G., Riegl, B., Yamano, H., & O'Leary, M. J. (2011).
424 Implications of reef ecosystem change for the stability and maintenance of coral reef islands.
425 *Global Change Biology*, *17*(12), 3679–3696. https://doi.org/10.1111/j.1365-
426 2486.2011.02523.x

427 Perry, C. T., Morgan, K. M., & Yarlett, R. T. (2017). Reef habitat type and spatial extent as
428 interacting controls on platform-scale carbonate budgets. *Frontiers in Marine Science*, *4*, 185.
429 https://doi.org/10.3389/fmars.2017.00185

Purdy, E. G., & Gischler, E. (2005). The transient nature of the empty bucket model of reef sedimentation. *Sedimentary Geology*, *175*(1), 35–47. https://doi.org/10.1016/j.sedgeo.2005.01.007

Reimer, P. J., Bard, E., Bayliss, A., Beck, J. W., Blackwell, P. G., Ramsey, C. B., et al. (2013). IntCal13 and Marine13 Radiocarbon Age Calibration Curves 0–50,000 Years cal BP. *Radiocarbon*, *55*(4), 1869–1887. https://doi.org/10.2458/azu_js_rc.55.16947

Santos, G. M., Moore, R. B., Southon, J. R., Griffin, S., Hinger, E., & Zhang, D. (2007). AMS 14C Sample Preparation at the KCCAMS/UCI Facility: Status Report and Performance of Small Samples. *Radiocarbon*, *49*(2), 255–269. https://doi.org/10.1017/S0033822200042181

Slota, P. J., Jull, A. J. T., Linick, T. W., & Toolin, L. J. (1987). Preparation of Small Samples for 14C Accelerator Targets by Catalytic Reduction of CO. *Radiocarbon*, *29*(2), 303–306. https://doi.org/10.1017/S0033822200056988

Southon, J., Kashgarian, M., Fontugne, M., Metivier, B., & Yim, W. W.-S. (2002). Marine Reservoir Corrections for the Indian Ocean and Southeast Asia. *Radiocarbon*, *44*(1), 167–180. https://doi.org/10.1017/S0033822200064778

Storlazzi, C. D., Elias, E. P. L., & Berkowitz, P. (2015). Many atolls may be uninhabitable within decades due to climate change. *Scientific Reports*, *5*, 14546. https://doi.org/10.1038/srep14546

Storlazzi, C. D., Gingerich, S. B., van Dongeren, A., Cheriton, O. M., Swarzenski, P. W., Quataert, E., et al. (2018). Most atolls will be uninhabitable by the mid-21st century because of sea-level rise exacerbating wave-driven flooding. *Science advances*, *4*(4), p.eaap9741. https://doi.org/10.1126/sciadv.aap9741

Stuiver, M., & Polach, H. A. (1977). Discussion Reporting of 14C Data. *Radiocarbon*, *19*(3), 355–363. https://doi.org/10.1017/S0033822200003672

Stuiver, M., & Reimer, P. J. (1993). Extended 14C Data Base and Revised CALIB 3.0 14C Age Calibration Program. *Radiocarbon*, *35*(1), 215–230. https://doi.org/10.1017/S0033822200013904

Tolman, H. L. (2009). *User manual and system documentation of WAVEWATCH III TM version 3.14.* (Technical note, MMAB Contribution No. v. 276) (p. 220).

459 UNDP. (2007). *Detailed Island Risk Assessment in the Maldives. Vol III detailed Island Reports,*
460 *G. Dh. Thinadhoo – Part 1*. Maldives: UNDP.

461 Woodroffe, C. D. (1993). Morphology and evolution of reef islands in the Maldives.
462 *Proceedings of the 7th International Coral Reef Symposium*, *2*, 1217–1226.

463 Woodroffe, C. D., & Morrison, R. J. (2001). Reef-island accretion and soil development on
464 Makin, Kiribati, central Pacific. *CATENA*, *44*(4), 245–261. https://doi.org/10.1016/S0341-
465 8162(01)00135-7

466 Woodroffe, C. D, McLean, R. F., Smithers, S. G., & Lawson, E. M. (1999). Atoll reef-island
467 formation and response to sea-level change: West Island, Cocos (Keeling) Islands. *Marine*
468 *Geology*, *160*(1), 85–104. https://doi.org/10.1016/S0025-3227(99)00009-2

469 Woodroffe, C. D., Samosorn, B., Hua, Q., & Hart, D. E. (2007). Incremental accretion of a sandy
470 reef island over the past 3000 years indicated by component-specific radiocarbon dating.
471 *Geophysical Research Letters*, *34*(3). https://doi.org/10.1029/2006GL028875

472 Young, I. R. (1999). Seasonal variability of the global ocean wind and wave climate.
473 *International Journal of Climatology*, *19*(9), 931–950. https://doi.org/10.1002/(sici)1097-
474 0088(199907)19:9<931::aid-joc412>3.0.co;2-o

Figure 1.

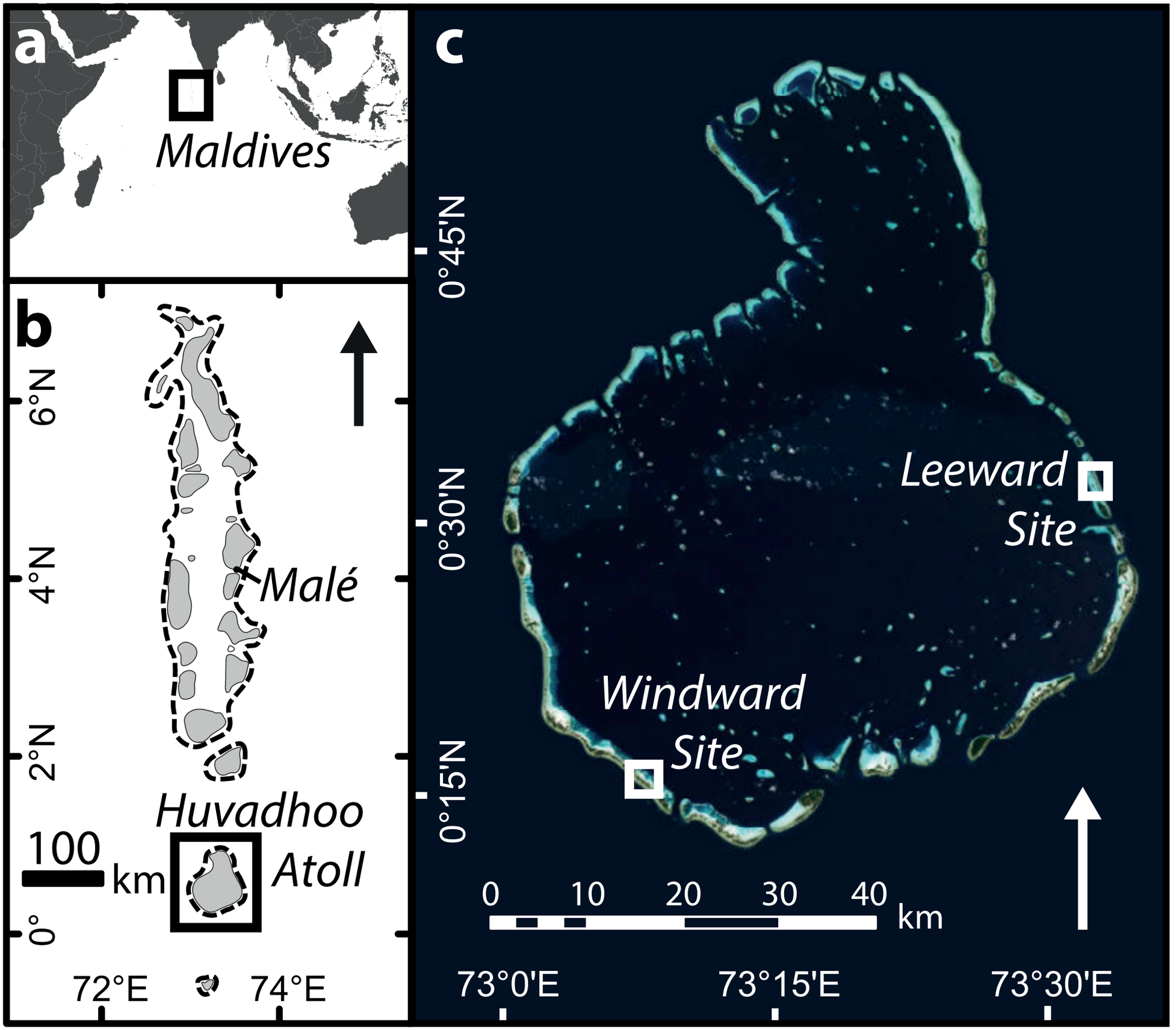
a
Maldives
b
6°N
4°N
2°N
0°
Malé
Huvadhoo
Atoll
100
km
72°E
74°E
c
0°45'N
0°30'N
0°15'N
Leeward
Site
Windward
Site
0
10
20
30
40
km
73°0'E
73°15'E
73°30'E

Figure 2.

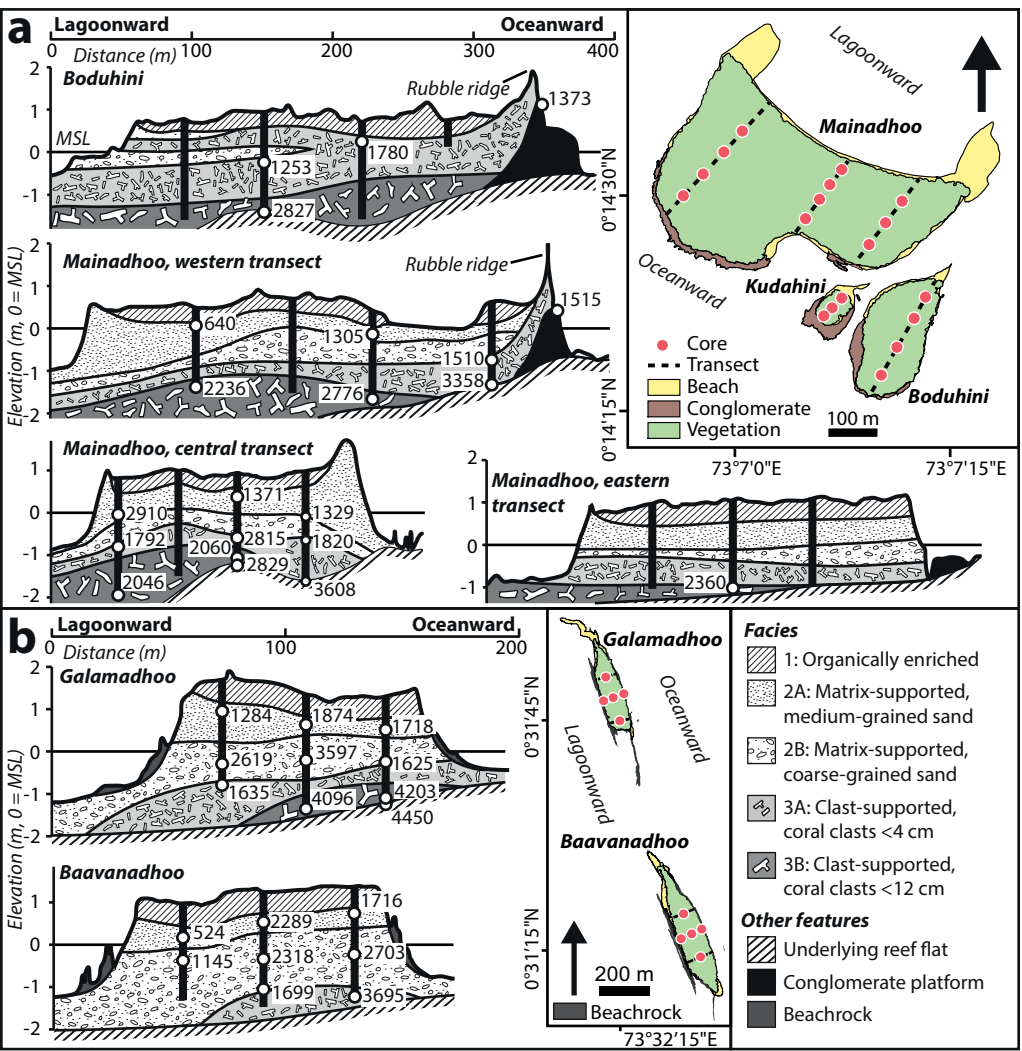
a
Lagoonward
Oceanward
Distance (m)
0
100
200
300
400
Boduhini
Rubble ridge
MSL
1373
1253
1780
2827
Mainadhoo, western transect
Rubble ridge
1515
640
1305
1510
3358
2236
2776
Elevation (m, 0 = MSL)
Mainadhoo, central transect
2910
1371
1329
1792
2815
1820
2060
2829
2046
3608
Mainadhoo, eastern transect
2360
Lagoonward
Mainadhoo
Oceanward
Kudahini
Boduhini
Core
Transect
Beach
Conglomerate
Vegetation
100 m
0°14'30"N
0°14'15"N
73°7'0"E
73°7'15"E
b
Lagoonward
Oceanward
Distance (m)
0
100
200
Galamadhoo
1284
1874
1718
2619
3597
1625
1635
4096
4203
4450
Baavanadhoo
1716
524
2289
2703
1145
2318
1699
3695
Galamadhoo
Oceanward
Lagoonward
Baavanadhoo
200 m
Beachrock
0°31'45"N
0°31'15"N
73°32'15"E
Facies
1: Organically enriched
2A: Matrix-supported, medium-grained sand
2B: Matrix-supported, coarse-grained sand
3A: Clast-supported, coral clasts <4 cm
3B: Clast-supported, coral clasts <12 cm
Other features
Underlying reef flat
Conglomerate platform
Beachrock

Figure 3.

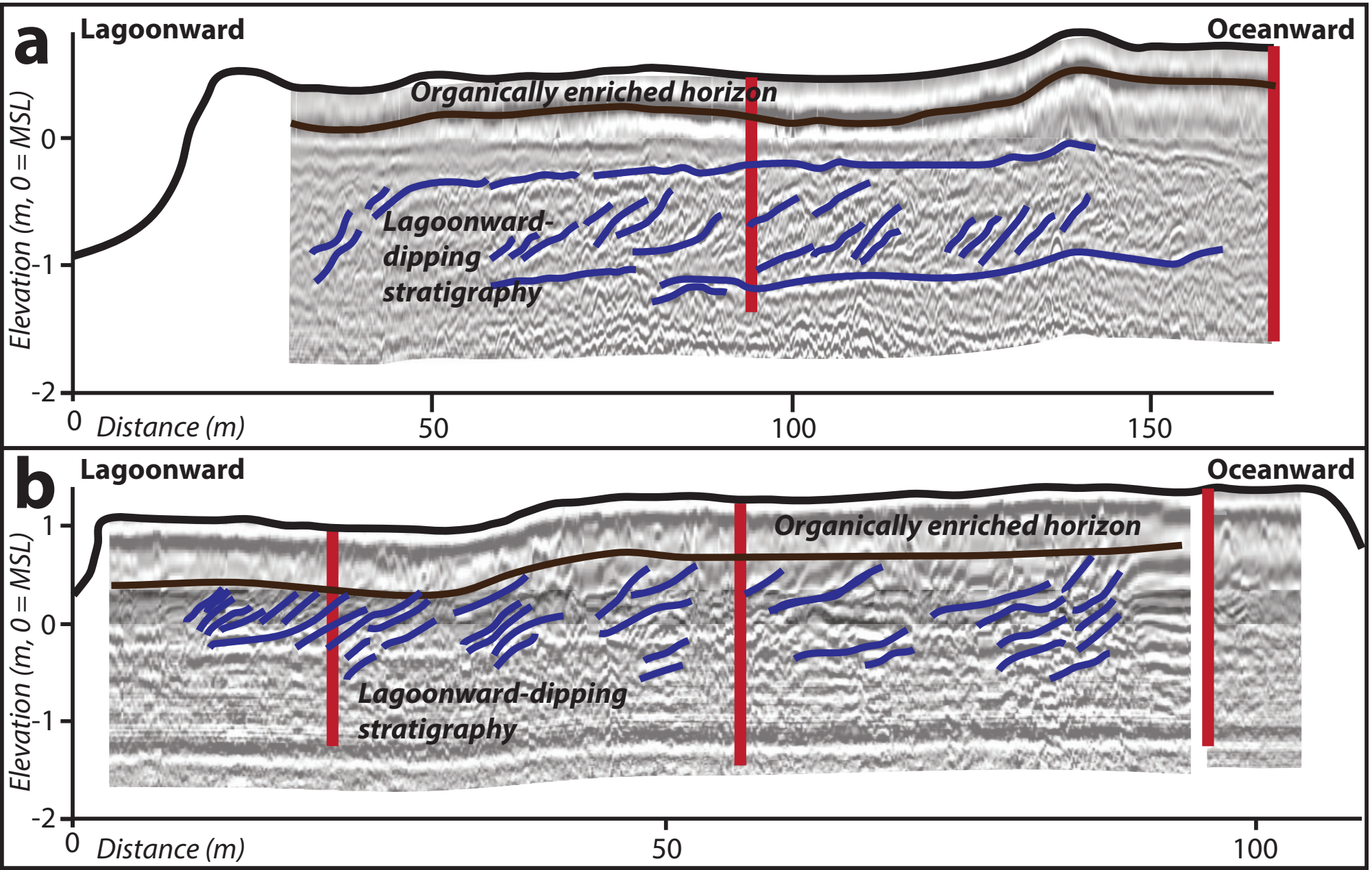
a
Lagoonward
Oceanward
Organically enriched horizon
Lagoonward-
dipping
stratigraphy
Elevation (m, 0 = MSL)
0
-1
-2
0
Distance (m)
50
100
150
b
Lagoonward
Oceanward
Organically enriched horizon
Lagoonward-dipping
stratigraphy
Elevation (m, 0 = MSL)
1
0
-1
-2
0
Distance (m)
50
100

Figure 4.

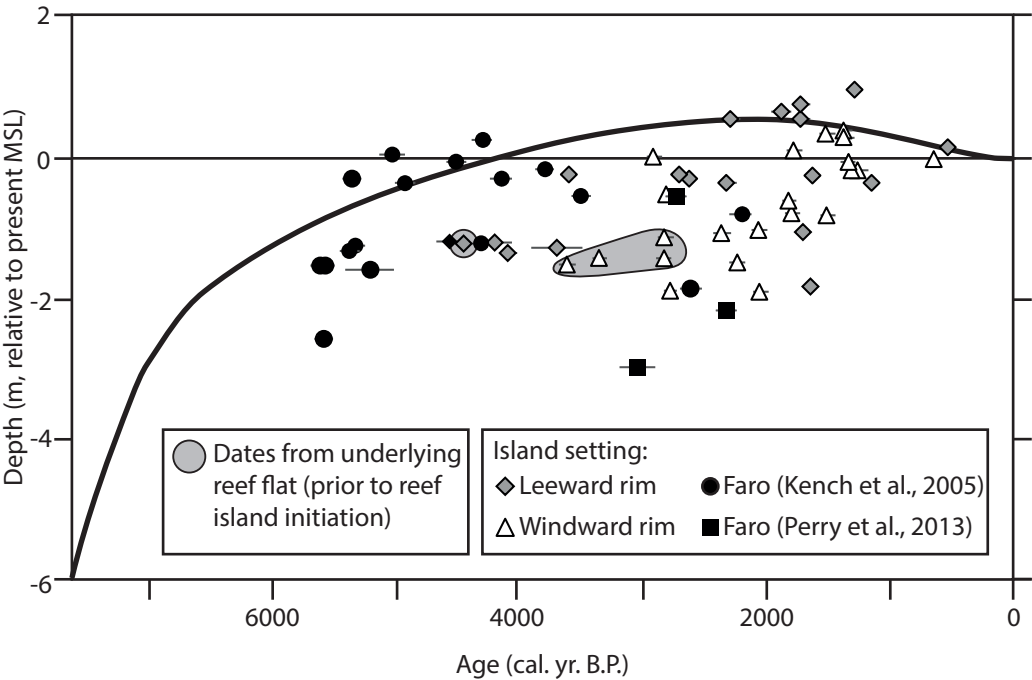
2
0
-2
-4
-6
Depth (m, relative to present MSL)
6000
4000
2000
0
Age (cal. yr. B.P.)
Dates from underlying reef flat (prior to reef island initiation)
Island setting:
Leeward rim
Windward rim
Faro (Kench et al., 2005)
Faro (Perry et al., 2013)

Figure 5.

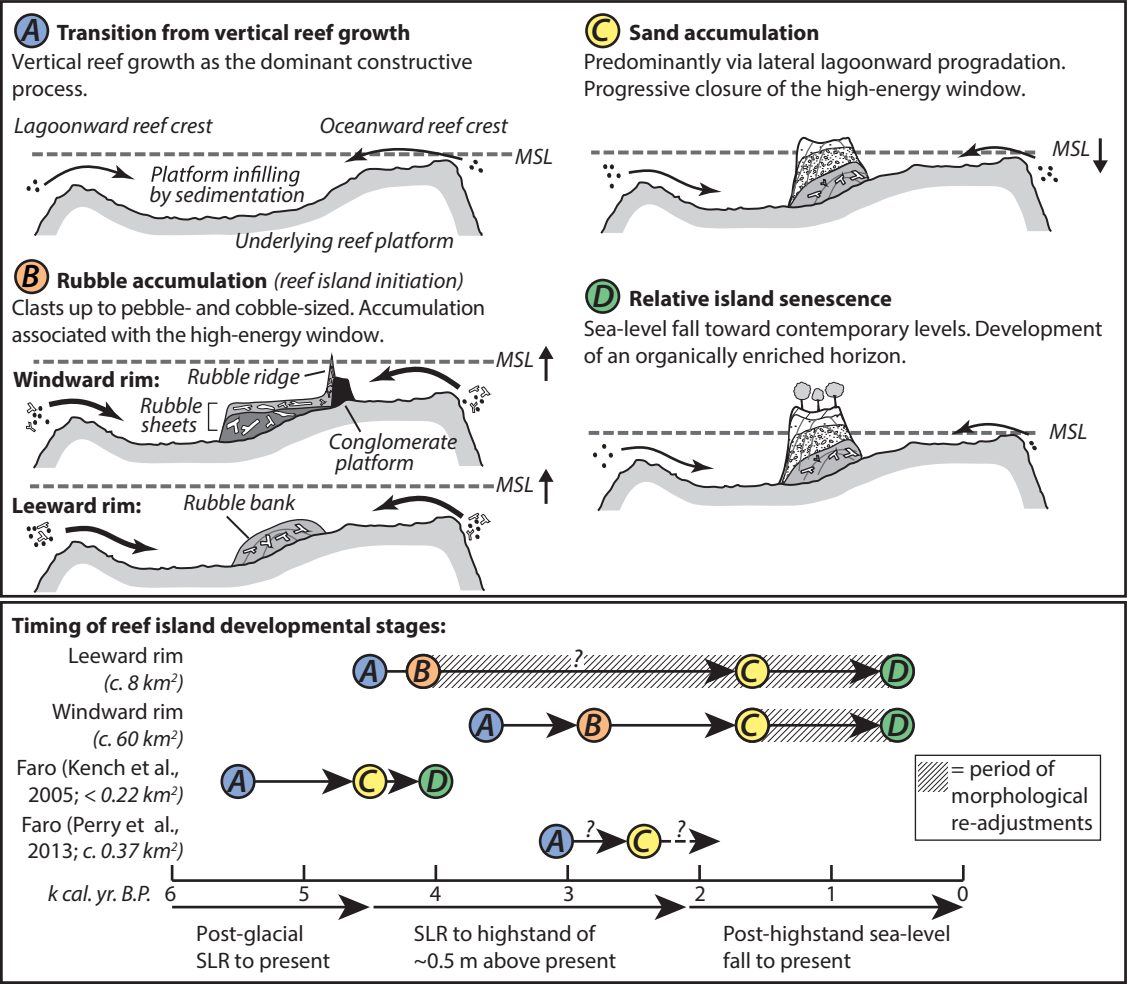
A Transition from vertical reef growth
Vertical reef growth as the dominant constructive process.
Lagoonward reef crest
Oceanward reef crest
MSL
Platform infilling by sedimentation
Underlying reef platform
B Rubble accumulation (reef island initiation)
Clasts up to pebble- and cobble-sized. Accumulation associated with the high-energy window.
Windward rim:
Rubble ridge
Rubble sheets
Conglomerate platform
Leeward rim:
Rubble bank
C Sand accumulation
Predominantly via lateral lagoonward progradation. Progressive closure of the high-energy window.
D Relative island senescence
Sea-level fall toward contemporary levels. Development of an organically enriched horizon.
Timing of reef island developmental stages:
Leeward rim (c. 8 km²)
Windward rim (c. 60 km²)
Faro (Kench et al., 2005; < 0.22 km²)
Faro (Perry et al., 2013; c. 0.37 km²)
= period of morphological re-adjustments
k cal. yr. B.P.
6
5
4
3
2
1
0
Post-glacial SLR to present
SLR to highstand of ~0.5 m above present
Post-highstand sea-level fall to present